Optimal PIDA Controller Design for Maglev Vehicle Suspension System by Lévy-Flight Firefly Algorithm

Sarot Hlangnamthip[1] Deacha Puangdownreong[2]*
[1]Department of Electrical Engineering, Faculty of Engineering
Southeast Asia University, 19/1 Petchakasem Rd., Nongkhaem, Bangkok, 10160
[2]Department of Electrical Engineering, Graduate School
Southeast Asia University, 19/1 Petchakasem Rd., Nongkhaem, Bangkok, 10160
*Corresponding author: Email: deachap@sau.ac.th
(Received: October 25, 2018; Accepted: February 15, 2019)

ABSTRACT

In modern vehicles, intelligent suspension systems have been widely applied with complex control algorithms. The suspension design problem aims to achieve a good suspension providing a comfortable ride and good handling within a reasonable range of road-profile deflection. In this paper, the proportional-integral-derivative-accelerated (PIDA) controller design for the magnetically levitated (Maglev) vehicle suspension system by the Lévy-flight firefly algorithm (LFFA), one of the most powerful metaheuristic optimization searching techniques, is proposed. For comparison with LFFA-based design approach, the results obtained by the PIDA controller will be compared with those obtained by the PI, PD and PID controllers. Simulation results show that the LFFA can provide optimal PIDA controller for a given suspension system. The PIDA controller yielded very satisfactory response superior to PI, PD and PID, respectively.

Keyword: PIDA controller, Maglev vehicle, suspension system, Lévy-flight firefly algorithm, modern optimization.

1. Introduction

In modern vehicles, a suspension system plays an important and imperative role in increasing the ride comfort. The main purpose of a suspension system is to provide a comfortable ride and good handling within a reasonable range of deflection or irregularity of road profile [1-3]. For high-speed transport links in modern economies, the magnetically levitated (Maglev) vehicles have been widely used in many countries. There are two most effective suspension methods, i.e electro-dynamic suspension (EDS) and electro-magnetic suspension (EMS) [4-6]. The former requires super-conducting materials to produce sufficient repulsive force to levitate a vehicle over a conducting track, while the later employs the attractive forces of sets of electromagnets acting upwards to levitate the vehicle towards the tracks [7-8]. Generally, the suspension system of the Maglev vehicles can be controlled by PD/PID controllers. Based on the modern optimization, designing of PD/PID controllers for Maglev vehicle suspension system by some potential metaheuristic algorithms has been developed, for example, by using genetic algorithm (GA) [9], evolutionary algorithm (EA) [10] and particle swarm optimization (PSO) [11].

In control theory, the proportional-integral-derivative-accelerated (PIDA) controller was developed and proposed by Jung and Dorf in 1996 [12]. It possesses three arbitrary zeros and one pole at origin. This leads the PIDA more benefit than the classical PID controller for higher-order plants. Designing of the PIDA controller by well-known metaheuristic algorithms has been launched, for instance, by GA [13], PSO [14], cuckoo search (CS) [15] and spider monkey optimization (SMO) [16].

By literature reviews, the firefly algorithm (FA) was firstly proposed in 2008 by Yang [17-18] based on the flashing behavior of fireflies and uniform distribution for randomly generating the feasible solutions. As one of the most efficient population-based metaheuristic algorithms, the FA was applied to almost every area of sciences and engineering, including power systems [19], image processing [20], antenna design [21], civil engineering [22], robotics [23], semantic web [24], chemistry [25], meteorology [26], wireless sensor networks [27], control engineering [28-29] and so forth.

In 2010, two years after the former version of the FA was initiated, the later version of FA named the Lévy-flight firefly algorithm (LFFA) was proposed by Yang [30]. The algorithm of LFFA was still based on the flashing behavior of fireflies, but Lévy-flight distribution is employed to randomly generate new solutions. The LFFA was tested against several nonlinear and multimodal standard test functions. Results obtained by the LFFA outperformed those by traditional algorithms including GA and PSO. The state-of-the-art and its applications of the LFFA have been reviewed and reported [31-32].

In this paper, the LFFA is applied to design an optimal PIDA controller for the Maglev vehicle suspension system. For comparison with LFFA-based design approach, the results obtained by the PIDA controller will be compared with those obtained by the PI, PD and PID controllers, respectively. After an introduction is provided in section 1, the remaining part of the paper is organized as follows. Modeling of Maglev suspension system is described in section 2. The LFFA-based PIDA design problem formulation is performed in section 3. Results and discussions are illustrated in section 4. Conclusions are given in section 5.

2. Maglev Suspension Model

The cross-section of a general Maglev vehicle is shown in Fig. 1(a), while its equivalent one-dimensional vehicle model with two-degrees-of-freedom is represented in Fig. 1(b), consisting of two lumped masses m_p and m_s, two linear springs k_p and k_s, and two viscous dampings b_p and b_s, representing primary (chassis) and secondary (passenger cabin) suspensions, respectively [5-6].

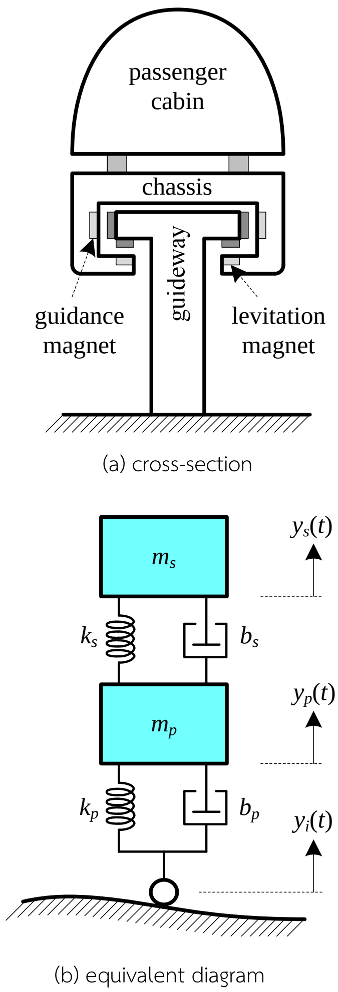

Fig. 1 Maglev vehicle suspension system

For the linear model, the equations of motion when the vehicle is at the equilibrium position are stated in (1) - (2).

$$m_p\ddot{y}_p + b_p(\dot{y}_p - \dot{y}_i) + k_p(y_p - y_i) - b_s(\dot{y}_s - \dot{y}_p) - k_s(y_s - y_p) = 0 \quad (1)$$

$$m_s\ddot{y}_s + b_s(\dot{y}_s - \dot{y}_p) + k_s(y_s - y_p) = 0 \quad (2)$$

From (1) and (2), the relation in (3) can be formulated, where y_p and y_s are positions of primary (chassis) and secondary (passenger cabin) suspensions, and y_i is disturbance from guideway irregularity.

$$m_p\ddot{y}_p + m_s\ddot{y}_s + b_p(\dot{y}_p - \dot{y}_i) + k_p(y_p - y_i) = 0 \quad (3)$$

The s-domain transfer functions of primary suspension $G_1(s)$ and secondary suspension $G_2(s)$ once considering guideway disturbance y_i as an input variable can be described in (4) and (5), respectively.

$$G_1(s) = \frac{Y_p(s)}{Y_i(s)} = \frac{\left(\begin{array}{l} m_s b_p s^3 + (m_s k_p + b_s b_p)s^2 \\ +(b_p k_s + b_s k_p)s + k_s k_p \end{array}\right)}{\left(\begin{array}{l} m_s m_p s^4 + [m_p b_s + m_s(b_p + b_s)]s^3 \\ +[m_p k_s + m_s(k_p + k_s) + b_s b_p]s^2 \\ +(b_p k_s + b_s k_p)s + k_s k_p \end{array}\right)} \quad (4)$$

$$G_2(s) = \frac{Y_s(s)}{Y_i(s)} = \frac{\left(b_s b_p s^2 + (b_p k_s + b_s k_p)s + k_s k_p\right)}{\left(\begin{array}{l} m_s m_p s^4 + [m_p b_s + m_s(b_p + b_s)]s^3 \\ +[m_p k_s + m_s(k_p + k_s) + b_s b_p]s^2 \\ +(b_p k_s + b_s k_p)s + k_s k_p \end{array}\right)} \quad (5)$$

The Maglev vehicle suspension model can be represented by the block diagram as shown in Fig. 2.

3. LFFA-Based PIDA Design Problem

In this section, algorithms of the original FA and the LFFA are briefly reviewed. Then, the LFFA-based PIDA controller design approach is elaborately described.

3.1 FA Algorithm

The original firefly algorithm (FA) was firstly developed by Yang in 2008 by [17-18] based on the flashing behavior of fireflies. The flashing light of fireflies is produced by a process of bioluminescence to attract mating partners (communication) and to attract potential prey. The FA's algorithm is developed from three idealized rules:

(i) fireflies are unisex so that one firefly will be attracted to other fireflies regardless of their sex;

(ii) the attractiveness is proportional to the brightness, and they both decrease as their distance increases. Thus for any two flashing fireflies, the less brighter one will

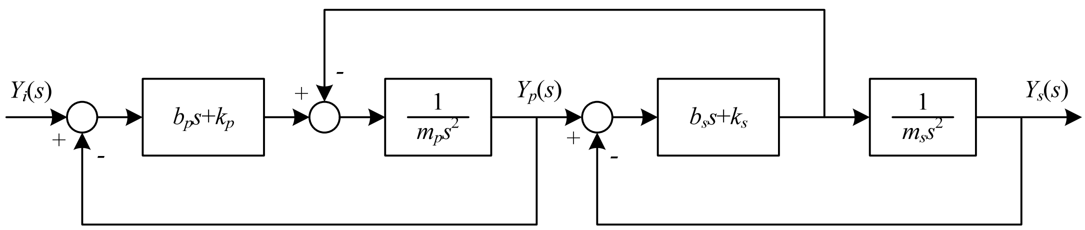

Fig. 2 Block diagram for two-degree-of-freedom Maglev vehicle model

move towards the brighter one. If there is no brighter one than a particular firefly, it will move randomly;

(iii) the brightness of a firefly is determined by the landscape of the objective function.

Based on these rules, the FA's algorithm can be summarized by the pseudo code shown in Fig. 3.

In FA, there are two important issues: the variation of light intensity and formulation of the attractiveness. The attractiveness of a firefly is determined by its brightness which in turn is associated with the encoded objective function. Along the distance *r*, the light intensity *I* varies according to the inverse square law $I(r) = I_s/r^2$, where I_s is the intensity at the source. For a given medium with a fixed light absorption coefficient, the light intensity *I* varies with the distance *r* as stated in (6), where I_0 is the original light intensity.

```
Objective function f(x), x = (x1,…,xd)^T
Generate initial population of fireflies xi = (i = 1, 2,…,n)
Light intensity Ii at xi is determined by f(xi)
Define light absorption coefficient γ
while (t < Max_Generation)
for i =1 : n all n fireflies
    for j =1 : i all n fireflies
      if (Ij > Ii)
        - Move firefly i towards j in d-dimension via
          uniformly distributed random
      end if
      - Attractiveness varies with distance r via exp[-γr]
      - Evaluate new solutions and update light intensity
    end for j
end for i
- Rank the fireflies and find the current best x*
end while
Report the best solution found
```

Fig. 3 Pseudo code of FA

$$I = I_0 e^{-\gamma r} \quad (6)$$

$$\beta = \beta_0 e^{-\gamma r^2} \quad (7)$$

$$r_{ij} = \|\boldsymbol{x}_i - \boldsymbol{x}_j\| = \sqrt{\sum_{k=1}^{d} (\boldsymbol{x}_{i,k} - \boldsymbol{x}_{j,k})^2} \quad (8)$$

The attractiveness of a firefly observed by adjacent fireflies is proportional to the light intensity. This can define the variation of attractiveness β with the distance *r* as expressed in (7), where β_0 is the attractiveness at $r = 0$. From parametric studies, $\beta_0 = 1$ is suggested for most applications [17-18]. The scaling factor γ in (6) and (7) is defined as the light absorption coefficient. In addition in (6) and (7), the distance r_{ij} between any two fireflies *i* and *j* at their locations x_i and x_j can be calculated by the Cartesian distance as expressed in (8), where $x_{i,k}$ is the k^{th} component of the spatial coordinate x_i of i^{th} firefly.

For an original FA, the movement of a firefly *i* is attracted to another more attractive (brighter) firefly *j* is determined by (9), where α_t is the randomization parameter, and ε_i is a vector of random numbers drawn from a Gaussian distribution or uniform distribution at time *t* [6]. In addition, α_t can be controlled during iterations as stated in (10), where α_0 is the initial randomness scaling factor, and δ is a cooling factor.

$$\boldsymbol{x}_i^{t+1} = \boldsymbol{x}_i^t + \beta_0 e^{-\gamma r_{ij}^2} (\boldsymbol{x}_j^t - \boldsymbol{x}_i^t) + \alpha_t \boldsymbol{\varepsilon}_i^t \quad (9)$$

$$\alpha_t = \alpha_0 \delta^t, \quad (0 < \delta < 1) \quad (10)$$

3.2 LFFA Algorithm

The Lévy-flight firefly algorithm (LFFA), the modified version of the FA, was proposed by Yang in 2010 [30]. Movement of a firefly *i* is attracted to another more attractive (brighter) firefly *j* is determined by (11), where the second term is due to the attraction while the third term is randomization via Lévy flights with α being the randomization parameter. The product

$\oplus$ means entrywise multiplications. The sign[rand-1/2] where rand $\in$ [0, 1] essentially provides a random sign or direction while the random step length is drawn from a Lévy distribution having an infinite variance with an infinite mean. From (11), a symbol Lévy(λ) represents the Lévy distribution as expressed in (12). The step length s can be calculated by (13), where u and v stand for normal distribution as stated in (14). Standard deviations of u and v are also expressed in (15). The algorithms of the LFFA can be represented by the pseudo code shown in Fig. 4.

$$\boldsymbol{x}_i^{t+1} = \boldsymbol{x}_i^t + \beta_0 e^{-\gamma r_{ij}^2}(\boldsymbol{x}_j^t - \boldsymbol{x}_i^t) + \alpha\,\mathtt{sign}\left[\mathtt{rand} - \frac{1}{2}\right] \oplus \text{Lévy}(\lambda) \quad (11)$$

$$\text{Lévy} \approx u = t^{-\lambda}, \quad (1 < \lambda \le 3) \quad (12)$$

$$s = \frac{u}{|v|^{1/\beta}} \quad (13)$$

$$u \approx N(0.\sigma_u^2), \quad v \approx N(0.\sigma_v^2) \quad (14)$$

$$\sigma_u = \left\{ \frac{\Gamma(1+\beta)\sin(\pi\beta/2)}{\Gamma[(1+\beta)/2]\beta 2^{(\beta-1)/2}} \right\}^{1/\beta}, \quad \sigma_v = 1 \quad (15)$$

```
Objective function f(x), x = (x1,…,xd)^T
Generate initial population of fireflies xi = (i = 1, 2,…,n)
Light intensity Ii at xi is determined by f(xi)
Define light absorption coefficient γ
while (t < Max_Generation)
for i =1 : n all n fireflies
    for j =1 : i all n fireflies
        if (Ij > Ii)
            - Move firefly i towards j in d-dimension via
              Lévy-flight distributed random
        end if
        - Attractiveness varies with distance r via exp[-γr]
        - Evaluate new solutions and update light intensity
    end for j
end for i
- Rank the fireflies and find the current best x*
end while
Report the best solution found
```

Fig. 4 Pseudo code of LFFA

3.3 LFFA-Based PIDA Controller Design

Regarding to the modern optimization, the LFFA-based optimal PIDA controller design for the Maglev vehicle suspension system can be represented by the block diagram in Fig. 5. The s-domain transfer functions of secondary suspension $G_2(s)$ in (5) will be used as a plant model $G_p(s)$ in Fig. 5. The plant model parameters, i.e., masses m_p and m_s, stiffnesses k_p and k_s, and dampings b_p and b_s for primary and secondary suspensions, are summarized in Table 1 [33-34].

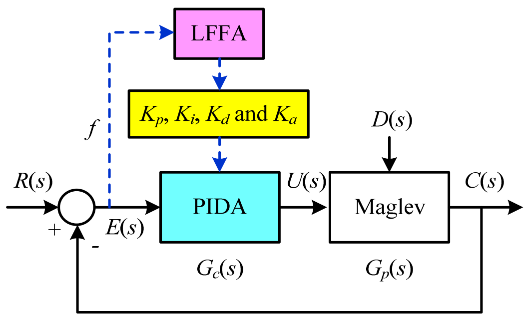

Fig. 5 LFFA-based PIDA design framework

Table 1 Maglev vehicle paramaters

Paramaters	Values
Primary suspension mass m_p	3.20×10^4 kg
Secondary suspension mass m_s	2.92×10^4 kg
Primary suspension damping b_p	1.13×10^6 N-s/m
Secondary suspension damping b_s	8.80×10^4 N-s/m
Primary suspension stiffness k_p	6.18×10^7 N/m
Secondary suspension stiffness k_s	7.37×10^5 N/m

The PI, PD, PID and PIDA controller models are stated in (16), (17), (18) and (19), respectively, where K_p is the proportional gain, K_i is the integral gain, K_d is the derivative gain and K_a is the accelerated gains. The sum-squared errors between reference position, r_j, and passenger cabin position, c_j, are set as the objective function $f(\cdot)$ stated in (20). As the constrained optimization, the time-domain response specification, consisting of the rise time (t_r), the maximum percent overshoot (M_p), the settling time (t_s) and the steady-state error (e_{ss}), is defined as the constrained functions as expressed in (21). Referring to Fig. 5, $f(\cdot)$ in (20) will be minimized by the LFFA in order to search for the appropriate values of K_p, K_i, K_d and K_a within their corresponding search spaces in (21).

$$G_c(s)\big|_{PI} = K_p + \frac{K_i}{s} \tag{16}$$

$$G_c(s)\big|_{PD} = K_p + K_d s \tag{17}$$

$$G_c(s)\big|_{PID} = K_p + \frac{K_i}{s} + K_d s \tag{18}$$

$$G_c(s)\big|_{PIDA} = K_p + \frac{K_i}{s} + K_d s + K_a s^2 \tag{19}$$

$$\text{Minimize} \quad f(K_p, K_i, K_d, K_a) = \sum_{j=1}^{N} (r_j - c_j)^2 \tag{20}$$

$$\text{Subject to} \quad \left.\begin{aligned} & t_r \le 0.05 \text{ sec}, \\ & M_p \le 10\%, \\ & t_s \le 0.10 \text{ sec}, \\ & e_{ss} \le 0.01\%, \\ & 0 \le K_p \le 100, \\ & 0 \le K_i \le 200, \\ & 0 \le K_d \le 10, \\ & 0 \le K_a \le 0.1 \end{aligned}\right\} \tag{21}$$

4. Results and Discussions

To design the PI, PD, PID and PIDA controllers for the Maglev vehicle suspension system, the LFFA algorithm was coded by MATLAB version 2018b (License No.#40637337). Search parameters of the LFFA are set according to Yang's recommendations [30], i.e. the numbers of fireflies n = 30, α_0 = 0.25, β_0 = 1, λ = 1.50 and γ = 1. In this work, 50 trails are searched to obtain the optimal PI, PD, PID and PIDA controllers. For all cases, the maximum generation (Max_Generation) = 200 is set as the termination criteria for each search trial.

4.1 Case-I (PI Controller)

In case of PI controller design with the LFFA-based design approach, the values of K_d and K_a in (21) will be fixed at zero. When the search process terminated, the optimal PI controller for the Maglev vehicle suspension system is obtained by the LFFA as expressed in (22). Fig. 6 shows the convergent rates of the objective function $f(\cdot)$ over 50 trials of the PI controller designed by the LFFA. The step responses of the Maglev vehicle suspension system without and with PI controller are depicted in Fig. 7.

$$G_c(s)\big|_{PI} = 9.7012 + \frac{14.9844}{s} \tag{22}$$

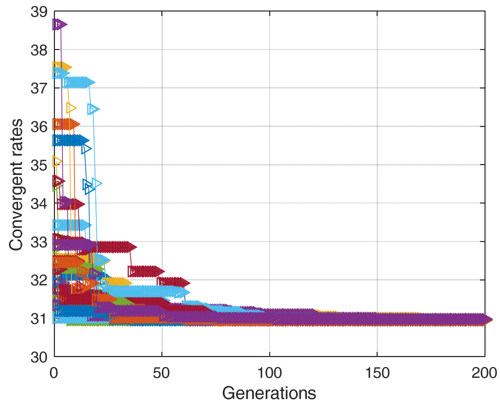

Fig. 6 Convergent rates of PI controller designed by LFFA

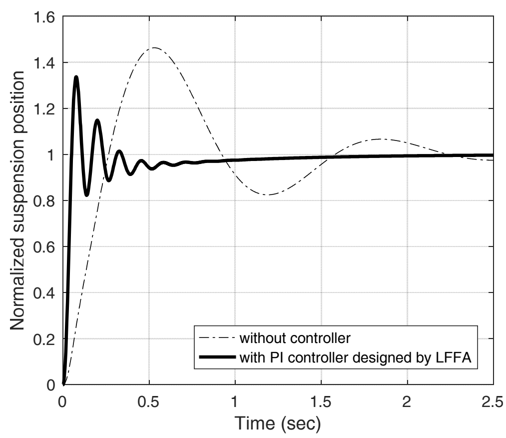

Fig. 7 Step responses of Maglev system without and with PI controller designed by LFFA

4.2 Case-II (PD Controller)

For the PD controller design with the LFFA-based design approach, the values of K_i and K_a in (21) will be fixed at zero. Once the search process stopped, the PD controller for the Maglev vehicle suspension system is optimized by the LFFA as stated in (23). The convergent rates of the objective function $f(\cdot)$ over 50 trials of the PD controller designed by the LFFA are plotted in Fig. 8. The step responses of the Maglev vehicle suspension system without and with PD controller are depicted in Fig. 9.

$$G_c(s)\big|_{PD} = 64.9937 + 3.0121s \qquad (23)$$

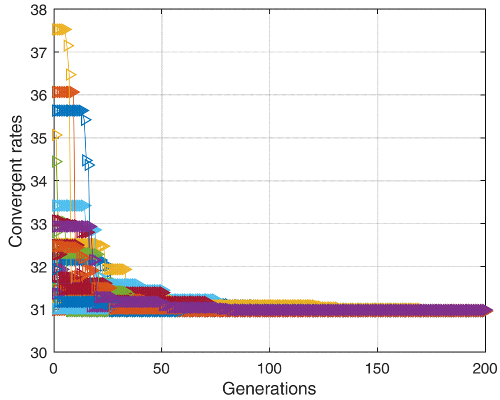

Fig. 8 Convergent rates of PD controller designed by LFFA

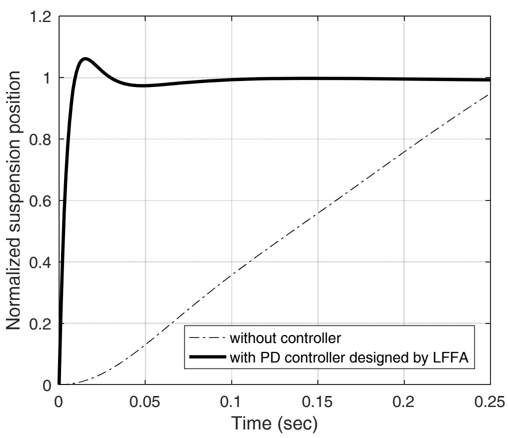

Fig. 9 Step responses of Maglev system without and with PD controller designed by LFFA

4.3 Case-III (PID Controller)

In case of PID controller design with the LFFA-based design approach, K_a in (21) is thus fixed at zero. When the search process stopped, the PID controller for the Maglev vehicle suspension system is optimized by the LFFA as stated in (24). The convergent rates of the objective function $f(\cdot)$ over 50 trials of the PID controller proceeded by the LFFA are plotted in Fig. 10. The step responses of the Maglev vehicle suspension system without and with PID controller are depicted in Fig. 11.

$$G_c(s)\big|_{PID} = 64.8045 + \frac{169.3762}{s} + 2.9871s \qquad (24)$$

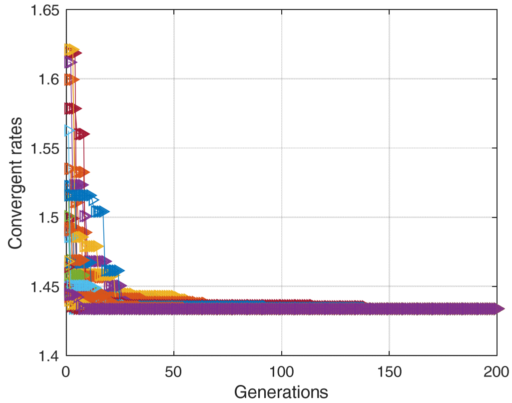

Fig. 10 Convergent rates of PID controller designed by LFFA

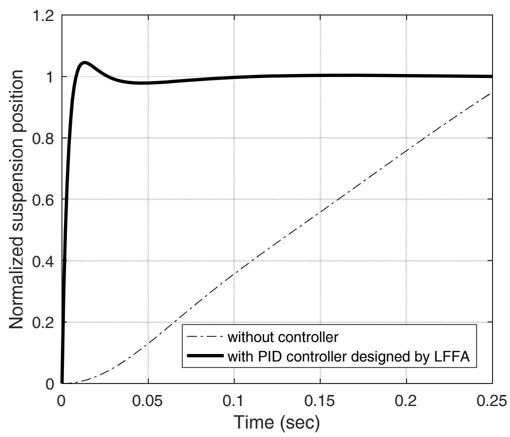

Fig. 11 Step responses of Maglev system without and with PID controller designed by LFFA

4.4 Case-IV (PIDA Controller)

Finally, for the PIDA controller design with the LFFA-based design approach, K_p, K_i, K_d and K_a are varied within their corresponding boundaries as given in (21). The optimal PIDA controller for the Maglev vehicle suspension system is obtained by the LFFA as stated in (25). The convergent rates of the PIDA controller design are plotted in Fig. 12. The step responses of the system without and with PIDA controller are depicted in Fig. 13.

$$G_c(s)|_{PIDA} = 65.1404 + \frac{179.1016}{s} + 5.7612s + 0.0002s^2 \quad (25)$$

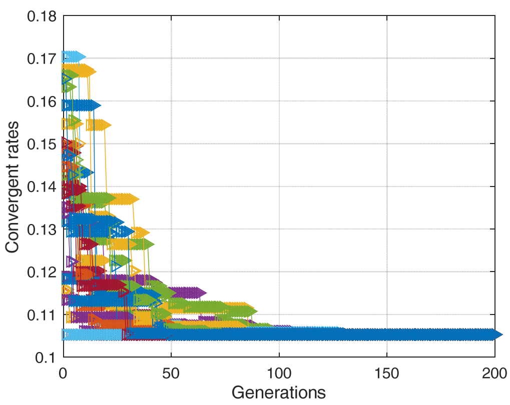

Fig. 12 Convergent rates of PIDA controller designed by LFFA

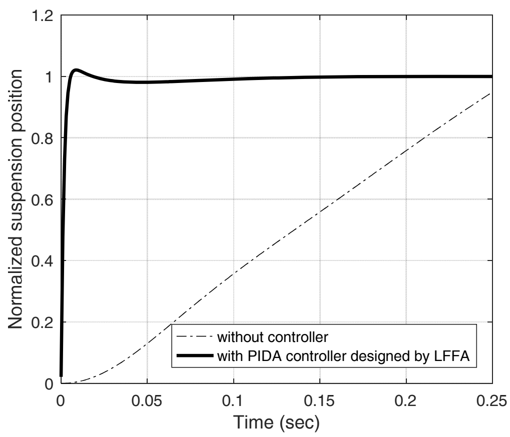

Fig. 13 Step responses of Maglev system without and with PIDA controller designed by LFFA

4.5 Result Comparison

All obtained results are summarized in Table 2. The step response of the Maglev vehicle suspension system without controller and with PI, PD, PID and PID controllers designed by the LFFA are depicted in Fig. 14. Referring to Table 2 and Fig. 14, it can be observed that the PI controller provides unacceptable response with slow and high overshoot and oscillation. The PD controller can improve transient responses, but it cannot eliminate the steady-state error of the system response. The PID can improve transient better than PD, and can eliminate the steady-state error as the PI. The PIDA outperforms PID controller in that it can improve transient response better than PID with faster and smoother, and can completely eliminate the steady-state error. The PIDA controller designed by the LFFA is optimal because the proposed objective function $f(\cdot)$ in (20) is completely minimized and the Maglev system response with the obtained PIDA corresponds to all preset constraint functions and search spaces in (21).

Fig. 15 shows the simulation results of the disturbance rejection of the Maglev system without and with PI, PD, PID and PIDA controller designed by LFFA. By comparison, it can be noticed that the effectiveness of the PIDA outperforms PI, PD and PID, respectively, due to the smallest and fastest disturbance rejection.

Table 2 Step-responses of Maglev suspension controlled systems

Controllers	Step-responses			
	t_r (sec.)	M_p (%)	t_s (sec.)	e_{ss} (%)
without	0.261	46.32	2.639	0.00
PI	0.049	33.72	1.162	0.00
PD	0.009	6.18	0.067	1.16
PID	0.008	4.54	0.055	0.00
PIDA	0.005	2.07	0.009	0.00

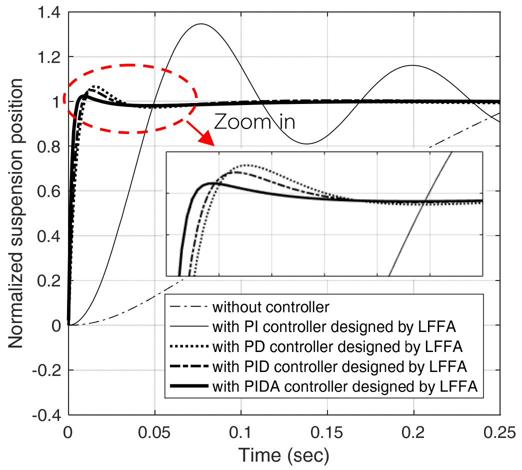

Fig. 14 Step responses of Maglev system without and with PI, PD, PID and PIDA controllers

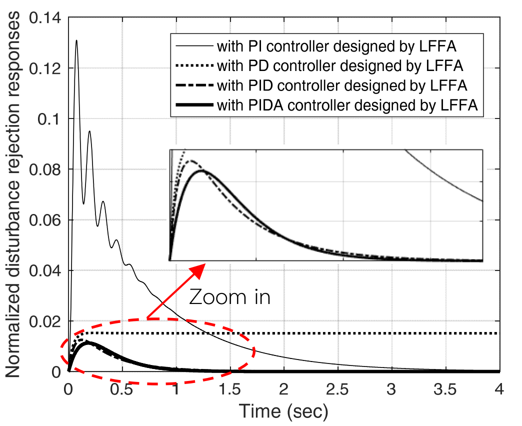

Fig. 15 Disturbance rejection responses of Maglev system without and with PI, PD, PID and PIDA controllers

5. Conclusions

Obtaining an optimal PIDA controller for Maglev vehicle suspension system based on the modern optimization design approach has been presented in this paper. As one of the most powerful metaheuristic algorithms, the LFFA has been applied to design an optimal PIDA controller for the given Maglev suspension system. With LFFA-based design approach, the results obtained by the PIDA controller have been compared with those obtained by the PI, PD and PID controllers. From Table 2 and Fig. 14, it can be investigated that the PI controller provides unacceptable response with slow and high overshoot and oscillation. Although the PD controller could improve transient response, it cannot eliminate the steady-state error. The PID controller could improve transient better than PD, and can eliminate the steady-state error like PI controller. Among those controllers, the PIDA controller outperformed PI, PD and PID controllers, respectively. The PIDA could improve transient response with faster and smoother than others, and can completely eliminate the steady-state error of the Maglev suspension controlled system responses. With the LFFA-based, the effectiveness of the optimal PIDA over PI, PD and PID has been confirmed by the smoothest and fastest responses of both step response and disturbance rejection as depicted in Fig. 14 and 15.

6. References

[1] R. S. Sharp and D. A. Crolla, "Road vehicle suspension system design - a review," *Vehicle Syst. Dynam.*, vol. 16, no. 3, pp. 167-192, 1987.

[2] A. Shirahatt, P. S. S. Prasad, P. Panzade and M. M. Kulkarni, "Optimal design of passenger car suspension for ride and road holding," *J. Braz. Soc. Mech. Sci. & Eng.*, vol. 30, no. 1, pp. 66-76, 2008.

[3] J. S. Lin and I. Kanellakopoulos, "Nonlinear design of active suspensions," *IEEE Control Syst. Mag.*, vol. 17, no. 3, pp. 45-59, 1997.

[4] D. S. Armstrong, "Magnet/rail systems - a critical review of the options," in *International Conference on Maglev Transport Now and for the Future*, St. John's Hotel, Solihull, UK., 1984, pp. 59-66.

[5] V. Zakian, *Control Systems Design: A New Framework*, London Limited: pringer-Verlag, 2005.

[6] Y. Cai, S. S. Chen and D. M. Rote, *Dynamics and Controls in Maglev Systems*, Argonne

National Laboratory, U.S. department of Energy, 1992.

[7] A. Butar and R. Sales, "Control for MagLev vehicles," *IEEE Control Syst*., vol. 18, no. 4, pp. 18-25, 1998.

[8] A. Charara, J. De Miras and B. Caron, "Nonlinear control of a magnetic levitation system without premagnetization," *IEEE Trans. Control Syst. Technol.*, vol. 4, no. 5, pp. 513-523, 1996.

[9] N. Katal and S. K. Singh, "Optimization of PID controller for quarter-car suspension system using genetic algorithm," *Int. J. Adv. Res. Comp. Eng. & Technol.*, vol. 1, no. 7, pp. 30-32, 2012.

[10] A. A. Aldair and W. J. Wang, "Design of fractional order controller based on evolutionary algorithm for a full vehicle nonlinear active suspension system," *Int. J. Control & Autom.*, vol. 3, no. 4, pp. 33-46, 2010.

[11] A. J. Qazi, C. W. De Silva, A. Khan and M. T. Khan, "Performance analysis of a semiactive suspension system with particle swarm optimization and fuzzy logic control," *Sci. World J.*, vol. 2014, pp. 1-12, 2014.

[12] S. Jung and R. C. Dorf, "Analytic PIDA controller design technique for a third order system," in *IEEE Conference on Decision and Control*, Kobe, Japan, 1996, pp. 2513-2518.

[13] S. Sornmuang and S. Sujitjorn, "GA-based PIDA control design optimization with an application to AC motor speed control," *Int. J. Math. & Comp. Simulat*., vol. 3, no. 4, pp. 67-80, 2010.

[14] D. Puangdownreong and S. Suwannarongsri, "Torsional resonance suppression via PIDA controller designed by the particle swarm optimization," in *The Annual International Conference Organized by Electrical Engineering/Electronics, Computer, Telecommunications and Information Technology*, Krabi, Thailand, 2008, pp. 673-676.

[15] A. Nawikavatan, T. Jitwang, C. Thammarat and D. Puangdownreong, "Application of cuckoo search to optimal PIDA controller design for three-tank liquid-level control system," in *International Conference on Engineering and Natural Science*, Sapporo, Hokkaido, Japan, 2018, pp. 51-59.

[16] A. Sharma, H. Sharma, A. Bhargava and N. Sharma, "Optimal design of PIDA controller for induction motor using spider monkey optimization algorithm," *Int. J. Metaheuristics*, vol. 5, no. 3/4, pp. 278-290, 2016.

[17] X. S. Yang, *Nature-Inspired Metaheuristic Algorithms*, Luniver Press, 2008.

[18] X. S. Yang, "Firefly algorithms for multimodal optimization, stochastic algorithms, foundations and Applications," *Lect. Notes Comp. Sci.*, vol. 5792, pp. 169-178, 2009.

[19] B. Rampriya, K. Mahadevan and S. Kannan, "Unit commitment in deregulated power system using Lagrangian firefly algorithm," in *IEEE International Conference on Communication Control and Computing Technologies*, Nagercoil, Tamil Nadu, India, 2010, pp. 389-393.

[20] T. Hassanzadeh, H. Vojodi and F. Mahmoudi, "Non-linear gray scale image enhancement based on firefly algorithm," in *The 2nd International Conference on Swarm, Evolutionary, and Memetic Computing,* Visakhapatnam, Andhra Pradesh, India, 2011, pp.174-181.

[21] B. Basu and G. Mahanti, "Thinning of concentric two-ring circular array antenna using firefly algorithm," *Sci. Iran.*, vol. 19, no. 6, pp. 1802-1809, 2012.

[22] S. Gholizadeh and H. Barati, "A comparative study of three metaheuristics for optimum design of trusses," *Int. J. Optim. Civil Eng.*, vol. 3, pp. 423-441, 2012.

[23] S. Severin and J. Rossmann, "A comparison of different metaheuristic algorithms for optimizing blended PTP movements for industrial robots," in *International Conference on Intelligent Robotics and Applications*, Montreal, QC, Canada, 2012, pp. 321-330.

[24] C. Pop, V. Chifu, I. Salomie, R. Baico, M. Dinsoreanu and G. Copil, "A hybrid firefly-inspired approach for optimal semantic web service composition," *Scalable Comp. Prac. & Exp.*, vol. 12, pp. 363-369, 2011.

[25] S. E. Fateen, A. Bonilla-Petriciolet and G. P. Rangaiah, "Evaluation of covariance matrix adaptation evolution strategy, shuffled complex evolution and firefly algorithms for phase stability, phase equilibrium and chemical equilibrium problems," *Chem. Eng. Res. & Des.*, vol. 90, no. 12, pp. 2051-2071, 2012.

[26] A. F. d. Santos, H. F. d. Campos Velho, E. F. Luz, S. R. Freitas, G. Grell and M. A. Gan, "Firefly optimization to determine the precipitation field on South America," *Inv. Prob. Sci. & Eng.*, vol. 21, no. 3, pp. 1-16, 2013.

[27] M. Breza and J. McCann, "Lessons in implementing bio-inspired algorithms on wireless sensor networks," in *IEEE NASA/ESA Conference on Adaptive Hardware and Systems*, Washington, DC., USA., 2008, pp. 271-276.

[28] O. Abedinia, N. Amjady, K. Kiani and H. Shayanfar, "Fuzzy PID based on firefly algorithm: load frequency control in deregulated environment," in *The 2012 International Conference on Bioinformatics and Computational Biology*, Varna, Bulgaria, 2012, pp. 1-7.

[29] D. Puangdownreong, S. Sumpunsri, M. Sukchum, C. Thammarat, S. Hlangnamthip and A. Nawikavatan, "FA-based optimal PIDA controller design for AVR system," in *The 2018 International Electrical Engineering Congress*, Krabi, Thailand, 2018, pp. 548-551.

[30] X.-S. Yang, "Firefly algorithm, Lévy flights and global optimization," *Res. & Dev. Intell. Syst.*, vol. XXVI, pp. 209-218, 2010.

[31] I. Fister, I. Fister Jr., X. S.Yang and J. Brest, "A comprehensive review of firefly algorithms," *Swarm. Evol. Comp.*, vol. 13, pp. 34-46, 2013.

[32] I. Fister, X. S. Yang, D. Fister and I. Fister Jr., "Firefly algorithm: a brief review of the expanding literature," *Cuckoo Search and Firefly Algorithm*, vol. 347, pp. 347-360, 2014.

[33] G. Bohn and H. Alscher, "The magnetic train transrapid 06," in *IEEE International Conference on Maglev and Linear Drives*, Piscataway, NJ., USA., 1986, pp. 233-242.

[34] G. Bohn and G. Steinmetz, "The electromagnetic suspension system of the magnetic train 'Transrapid'," in *The 7th International Conference on Maglev Transport*, Tokyo, Japan, 1985, pp. 107-114.